Society for Science and Education
United Kingdom

ISSN: 2055 - 1266
Volume 3 No 5
October 2016

Journal of Biomedical Engineering and Medical Imaging

TABLE OF CONTENTS

EDITORIAL ADVISORY BOARD

DISCLAIMER

All the contributions are published in good faith and intentions to promote and encourage research activities around the globe. The contributions are property of their respective authors/owners and the journal is not responsible for any content that hurts someone's views or feelings etc.

SOCIETY FOR SCIENCE AND EDUCATION
UNITED KINGDOM

JBEMi JOURNAL OF BIOMEDICAL ENGINEERING AND MEDICAL IMAGING

ISSN : 2055-1266
VOLUME 3 NO. 5

Wound Healing Assessment Using Digital Photography: A Review

Hamidreza Mohafez[1], Siti Anom Ahmad[1], Sharifah Ahmad Roohi [2] and Maryam Hadizadeh[3]

[1]Department of Electrical and Electronic Engineering, Faculty of Engineering, Universiti Putra Malaysia, Selangor, Malaysia;

[2]Department of Orthopaedics, Faculty of Medicine and Health Sciences, Universiti Putra Malaysia, 43400 UPM Serdang, Selangor, Malaysia;

[3]Department of Sport Studies, Faculty of Educational Studies, Universiti Putra Malaysia, 43400 UPM Serdang, Selangor, Malaysia;

hamidrezamohafez@gmail.com; sanom@upm.edu.my; roohihandsurgery@gmail.com; m.hadizadeh.sport@gmail.com

ABSTRACT

Digital photography as a non-invasive, simple, objective, reproducible, and practical imaging modality has been investigated for the wound healing assessment over the last three decades, and now has been widely used in clinical daily routine. Advances in the field of image analysis and computational intelligence techniques along with the improvements in digital camera instrumentation, expand the applications of standardized digital photography in diagnostic dermatology such as evaluation of tumours, erythema, and ulcers. A series of digital images taken at regular intervals carries the most informative wound healing indexes, color and dimension, that may help clinicians to evaluate the effectiveness of a particular treatment regimen, to relieve patient discomfort, to globally assess the healing kinetics, and to quantitatively compare different therapies; however, the extent of underlying tissue damage cannot be fully detected. This paper is an introductory review of the important investigations proposed by researchers in the context of clinical wound assessment. The principles of wound assessment using digital photography were shortly described, followed by review of the related literature in four main domains: wound tissue segmentation, automated wound area measurement, wound three dimensional (3D) analysis and volumetric measurement, and monitoring and evaluation of wound tissue changes during healing.

Keywords: Wound Assessment, Digital Photography, Image Analysis, Wound Healing

1 Introduction

Wound assessment at regular intervals helps clinicians to evaluate the effectiveness of adopted treatment strategy and change it if necessary; however it is complex and multi-sided which includes wound appearance, identification of factors delaying healing, wound etiology, monitoring and prediction of healing rates, and wound documentation [1]. The gold standard is the wound biopsy which provides valuable superficial and depth information with the cost of increasing the wound area and impairment in the healing process [2]. In clinical arena, assessment methods have mainly been based on

DOI: 10.14738/jbemi.35.2203
Publication Date: 12th September 2016
URL: http://dx.doi.org/10.14738/jbemi. 35.2203

measuring the two informative characteristics of the wound: dimension and colour [3]. The earliest methods used rulers, acetate sheets and alginate casts to measure the wound area and volume. However, the problem of direct contact to the wound, along with the poor precision due to subjective aspects of the measurement, made them less reliable [4]. In addition, automatic wound healing assessment, especially wound dimensional measurement would reduce the professionals' workload and costs, and improve the quality of patients' care [5]. Various simple and complex non-contact methods such as stereo-photogrammetry and structured light analysis were developed to reduce the measurement error rate to 0-3% and 3-5% respectively, to prevent wound contamination and to remove patient discomfort [6]. On the other hand, wound colorimetry which is based on the Red-Yellow-Black model, takes into account the ulcer's colour characteristics as a function of its clinical stage; however, it is more a measure of the clinicians' skills at cleaning up a wound than of the healing progress [7].

Significant advances in the field of digital image processing make the standardized digital photography as the most popular tool which considers both aspects of the wound for assessment of healing. Several successful attempts to classify wound tissue have been made through segmentation algorithms applied to various sets of features extracted from different colour spaces, with the aim of objectively monitoring the colour changes during healing [8-15] and automatically determining the wound volume and area [16-18]. All these proposed methods for assessing wound healing provide information only at the surface level and cannot be applied to all types of wound [2, 19]. This issue becomes more significant when dealing with chronic wounds such as diabetic foot ulcers (DFUs) which are notably different from acute wounds in that they can develop superficially or from within the deep tissue, depending on the nature of dominant risk factors [20]. This paper shortly describes the principles of digital photography, reviews the related studies that investigated the application of optical imaging in wound assessment, and enumerates limitations.

2 Clinical Assessment of Wound Healing

A thorough assessment of wound tissue should consider the following characteristics: size of the wound, edge of the wound, wound bed and colors, wound depth, surrounding skin, wound exudate, infection, and severity of pain. However, there is no universally established instrument applicable for all types of wounds which considers all above mentioned characteristics and satisfies all aspects of instrument validity, reliability, and measurement sensitivity. The quantitative assessment of chronic wounds still builds upon manual techniques and visual inspection to portray the wound physical appearance and the nature of tissues paved the wound bed [21, 22]. In practice, a wound is inspected on a weekly or fortnightly basis during replacement of dressing. The size of a healing wound tends to be reduced over time, while it is static or increasing in a deteriorating or non-healing wound [16]. Therefore, continuous measurement of wound size as a key indicator of healing and comparison of the recent wound's dimension with the current measurement may increase the likelihood of adopting effective treatment regimen, provide objective form of evaluation, help predict healing, enhance quality of patient care, contribute to more accurate communications between professionals, and enhance overall wound management [3, 16, 23-25]. Of the several contact and non-contact methods proposed for wound dimensional measurement, ruler based technique, transparent tracing, and computer assisted planimetry are most commonly used in clinical daily routine [16, 26, 27]. The modified ruler technique is simple, fast, and cheap, while its poor precision (25%) for wound with complex shape along with risk of

infection made it less reliable [4, 28]. Tracing is a more accurate 2D method for wound with irregular shape in which the wound is outlined on a transparent squared acetate sheet and next the wound area is calculated by manually counting the amount of included squares; however, it is a tedious task and has shown poor inter-rater reliability [27, 29, 30]. In addition, the problem of steam forms below the film blocks the visibility of wound's outline; increases the risk of cross-contamination and patient's discomfort [30]. So, the digital planimetry was proposed to speed up the area calculation through using a digital tablet wherein the tracing is placed on it and the border is outlined by a stylus pen. It is well documented that the results of acetate tracing and the digital planimetry are in agreement for wounds with an area < $10cm^2$, while significant difference was reported for larger wounds. Moreover, using the second tracing automatically increases the error rate [27]. Colour also is an important parameter in wound care for two reasons: Firstly, wound colour may be used to classify wound tissue types (i.e. granulation, slough, and necrotic), guiding medical decisions like the type of dressing and prediction of possible complications; secondly, colour has been one way of identifying basic symptoms of inflammation [8]. The Red-Yellow-Black (RYB) model [31] is the commonly accepted tissue classifying method on the basis of colour used by clinicians and wound nurses, and is not limited to any specific wound type, such as pressure or diabetic foot ulcers. However, it is highly related to clinician's experience, time consuming, and irritating for patients. Advancement in the field of colour image processing along with advent of relatively cheap high quality compact digital camera, give rise to developing numerous 2D digital image analysis techniques for wound healing assessment. Here, the principles of digital imaging were described and the most successful attempts for area measurement and wound tissue classification using optical imaging were reviewed briefly.

3 Principles of Digital Imaging

Colourimetry, the measurement of colour, is a complex task. Ideally, a system with precisely known characteristics able to acquire images under exactly reproducible conditions is needed. Unfortunately it is very difficult to have perfect control over every aspect of the acquisition process like camera position and setup, lighting, and filters. Care has therefore to be exercised in order to eliminate as many variables as possible from the image acquisition process. Furthermore it is important that the images resulting from the acquisition process are of the highest quality and reveal as much information as possible about the problem at hand. Otherwise a range of post-acquisition digital image conditioning and filtering processes like noise reduction and colour correction may have to be used unnecessarily and it may become impossible to extract the required information [8]. An ideal image acquisition system consists of several sub-components (e.g. lighting box and filters) which are bulky and expensive; so, a single set of device including digital camera and colour checker would be used in case of achieving colour consistency by defining a protocol wherein all influential factors are specified and controlled as much as possible (Figure 1).

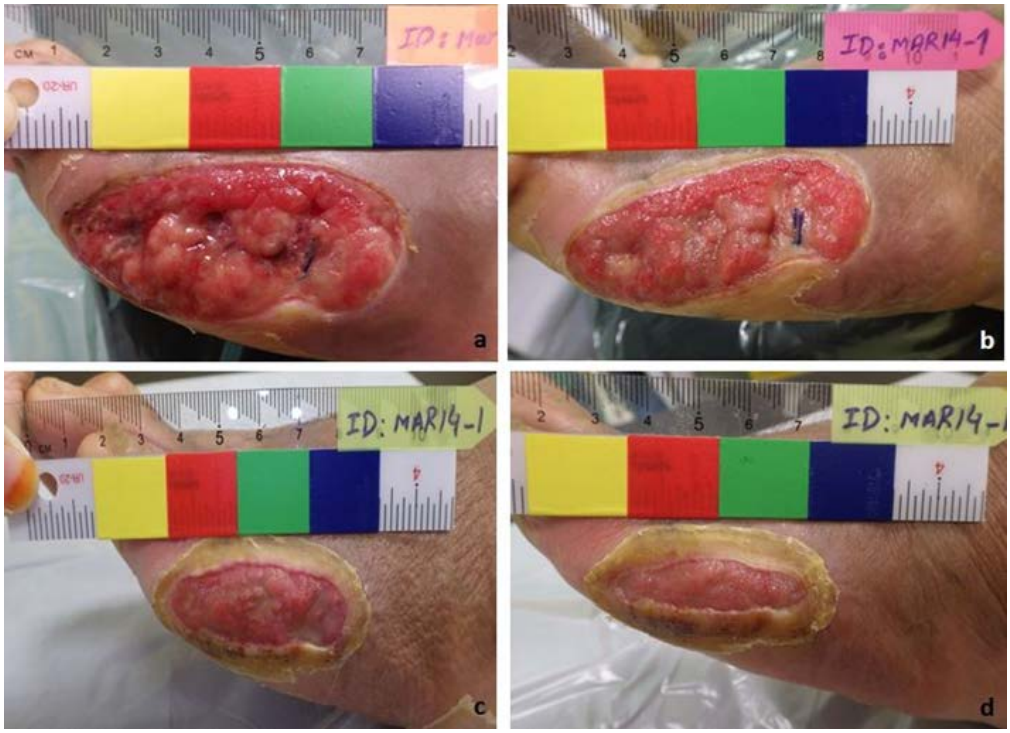

Figure 1. Optical images of a diabetic foot ulcer taken on (a) Day 7, (b) Day 14, (c) Day 21, and (d) Day 28 post-debridement in a controlled environment. As the wound images were taken under similar conditions with the same set of equipment, their colour characteristics were consistent and the subsequent colour corrections would be minimized.

4 Optical Imaging in Wound Assessment

Applications of digital photography in quantitative wound assessment can be categorized to four main domains: wound tissue classification, automated wound area measurement, wound three dimensional (3D) analysis and volumetric measurement, and monitoring and evaluation of wound tissue changes during healing.

4.1 Wound Tissue Classification using Digital Image Analysis

Tissue classification over the wound delineated from the image background, has been reported to be a complicated task. It is due to nature of the wounds with non-uniform combination of red granulation, black necrotic and yellow slough tissues that leads to colour ambiguity [10, 11, 32, 33]. Several successful attempts have been made to classify wound tissue through using segmentation algorithms applied to various sets of features extracted from different colour spaces, with the aim of objectively monitoring the colour changes during healing [5, 8-12, 14, 15, 32, 34-37]. Here, we tried to briefly review the most prominent investigations.

In a novel technique, the 3D RGB colour histogram was used for wound tissue classification, i.e. after computation of 3D RGB histogram of the manually delineated wound, a clustering technique was applied to cluster the histogram bins which lead to segmentation of the different tissue types within the wound site. Finally, segmented granulation tissue area was used as a quantitative measure for wound healing assessment [38]. Although the classification results were promising, the used un-calibrated wound image and insufficient number of wound images prevented the investigator from establishing

colour reproducibility and generalizing the proposed method. Moreover, reducing resolution of the RGB image, the way of selecting the seeds, and the order wherein the clusters created restricted the algorithm.

In another study, the slough tissue in 30 pressure ulcers was segmented and graded based on the hue value changes in HSI colour space after wound delineation performed by a semi-automatic method called adaptive spline technique, followed by calculation of amount of slough as a quantitative measure in wound healing assessment. The accuracy of colour assessment was compared with the clinicians' decision and 75% agreement was reported. However, it was concluded that the wound assessment just by optical images looks insufficient for clinicians as they normally consider the other parameters like pain, surrounding tissue, and wound odour. Also, the uncontrolled lighting condition appeared as 10% shift in red patches of colour checker which affected the reliability of the results for describing the minor changes in hue [9]. Meanwhile, the same team of researchers launched another study with the same protocol, but increasing the number of leg ulcers to 50. The results revealed that the red patches colour shift increased to 17%; so, calibration of hue values prior to wound analysis was suggested [12].

Three other investigations were used the support vector machine (SVM) for tissue classification in calibrated wound images. Firstly, Belem [8] studied the relationship between wound colour and inflammation that may be resulted from an infection. The manually delineated wound was automatically segmented in CIE L*u*v* into smaller regions, separating "healthy" and "non-healthy" tissues. Then, extracted statistical parameters were imposed to "brute force" approach to select the most successful ones for subsequent classification. Logistic regression (LR), support vector machine (SVM), and an artificial neural network (ANN) were utilized as classification engines which were compared against each other and the clinician's classification using the Kappa agreement estimator. Results demonstrated that SVM was the best performing classifier with more consistency in its judgment than most of the clinicians. The study outcomes were encouraging, but more information was required to guarantee causality between actual wound inflammation status and classification as the infection is not necessarily the sole cause.

In the second research, Automatic segmentation of wound region was performed using multi-dimensional histogram sampling technique that provided efficient set of feature vectors for as an input for SVM classifier. It was concluded that 3D colour histogram sampling, produced more discriminatory set of features for SVM classifier than those of one dimensional histogram which improved the accuracy of wound area segmentation by 20-30% [10]. However, such an approach failed to generate a contour as fine as the manual one traced by clinicians.

In the third study, the wound images were imposed to an unsupervised segmentation method before classification to increase the robustness of tissue labelling. Then the colour and texture descriptors (i.e. average, standard deviation, skewness, and kurtosis) were calculated in perceptually uniform colour spaces La*b* and LC*h* to design a SVM classifier with 88% successive overlapping scores. Finally, the unsupervised segmentation method was applied on test-samples, followed by classifying the regions. The results indicated that the classification performance was 75% and 60% for granulation and slough tissues respectively [33]. However, the classification error was greater than 50% for necrosis and the proposed approach required preliminary manual region of interest selection [14].

Zheng, Bradley [32] proposed a new technique to classify the wound bed tissues in leg ulcers using three 2D histograms of RGB pixel distribution values as an input for case-based retrieval , KNN classifier. The outcomes demonstrated that for binary classification, the accuracy ranged 86.2-99.45%, while for multi-class segmentation was 87.2%, higher than 77.6% obtained in study performed by [38].

Galushka, Zheng [5] used eighteen texture features extracted from co-occurrence matrix of each RGB channel and eighteen RGB colour features as an input for case-based classifier (CBR) to identify wound tissues. Two groups of experiment (i.e. three and six classes) were recruited to assess the accuracy. The results indicated that the textural features were less effective in multi-class segmentation, 58.3% and 54.4% accuracy for 3-class and 6-class respectively, than the colour features with accuracy of 89.93% and 86.8%. Such a drawback was due to the small size of region of interest which inevitably reduced the accuracy of classifier.

A hybrid design based on Bayesian classifiers and neural networks was used for automatic tissue classification in wound images. A region-growing approach and a mean shift strategy were designed for effective region segmentation wherein texture and color features were extracted. Then, a set of *k*-multilayer perceptrons was trained with inputs consisting of texture and color patterns, and outputs consisting of categorical tissue classes were determined by clinical experts. At the end, a Bayesian committee machine was formed by training a Bayesian classifier to integrate the classifications of the *k* neural networks, and the results of the classifications were improved using specific heuristics based on the wound topology. The results of binary cascade strategy showed the highest classification accuracy rate by specificity = 94.7%, accuracy = 91.5%, and average sensitivity = 78.7% [14]. Except granulation tissue, there were significant differences in sensitivity among the proposed approaches to classify the other tissue types, made each approach more or less appropriate to classify a particular tissue type.

A database including 74 different chronic wounds was imposed to Bayesian and SVM classifiers for automatic tissue classification. Firstly, the recorded RGB wound images were converted to HSI color space, followed by wound delineation through fuzzy-divergence-based thresholding. Then, set of color and texture features were selected as an input for aforementioned classifiers. The research outcomes revealed that the SVM showed higher accuracy for slough, granulation, and necrotic tissues by 90.47%, 86.94%, and 75.53%, respectively [11].

4.2 Wound Area Measurement Using Digital Photography

Digital photo planimetry has become increasingly popular for wound healing assessment wherein series of well-obtained digital images taken from the same region of an ulcer along with dimensional measurements can be applied as a yardstick to monitor the effectiveness of a treatment strategy [3, 4, 39-41]. In the context of wound's perimeter, area, and volume measurement, delineation in which details of the surrounding area is isolated from the wound information, is one the most important image processing steps; however, there is no single algorithm in existence that works perfectly for all types of wounds due to "the nature of the wounds". Manual delineation is tedious and is liable to two major criticisms: bias measurements and repeatability through using several observers [16]; therefore, several automated and semi-automated methods were developed to define the region of interest (ROI). The fully automated approaches failed to show acceptable performance as single algorithm cannot deal with all affecting factors like shape and type of wound, definition of wound edges, and type of dressing. So,

numerous semi-automatic algorithms which require some user interaction were proposed: active contour modelling [16, 42], contour detection using histogram segmentation [10], region growing for edge detection [43], clustering approaches [44], and texture analysis [16, 44, 45]. Once the wound boundary has been outlined, the circumference and area are measured in terms of lengths and pixel areas, respectively. Here, the most successful attempt for area measurement was reviewed shortly.

The most successful method was based on a Snake active contour model proposed by Jones and Plassmann [16] in which the manual delineation was adjusted as the initial solution and the final contour was obtained using piece-wise B-spline arcs and minimax principle. Despite of the fact that it produced significant results; it is very complex and failed in case of wounds with vague boundaries and existence of red and dark spots near the inner and outer sides of wound edges, is not robust against small changes in lighting, and any artefacts like shadow or piece of dressing in the image can also upset such a system.

As a result, manual wound delineation through using simple and fast software equipped with accurate scaling mechanism is still the first choice of professionals in everyday clinical routine. For instance, a digital planimetry software called Pictzar was developed using calibrated optical images and its accuracy, intra and inter-rater reliability was assessed on a database consisted of 200 images of the wounds with varying aetiologies. The accuracy and reliability mean value for small wounds (<4cm^2) were reported as 98% and 94% respectively [30].

4.3 Wound 3d Analysis And Volume Measurement

Despite of valuable information obtained from 2D measurement of wounds, it is insufficient for comprehensive assessment of wound healing and for detection of deep tissue changes. Moreover, area measurements do not show initial changes in deep ulcers wherein the healing improves by growth of granulation tissue from the wound's bed [29]. Traditional measurement of wound volume is limited to estimation of wound depth using sterile cotton tip and combine with area information through mathematical formula, filling the wound with saline and measuring the volume of the saline dispensed from syringe, and applying wound mould made of silicon rubber and weighing alginate moulds. These approaches increase the rate of contamination; and are inaccurate with error rate 10-40% and 5-15% for depth estimation using the cotton tips and wound moulds, respectively [46-48]. Several approaches tried to develop non-invasive volume measurement applying wound 3D reconstruction including photogrammetry [39, 49], structured light analysis [4, 17, 34, 50], and industrial 3D digitiser [18, 51].

4.3.1 Wound 3d Analysis Using Stereo-Photogrammetry

Wound stereo-photogrammetry was introduced by Bulstrode, Goode [28] where the wound depth was obtained by capturing the wound images in two different angles, followed by a matching algorithm trying to find the corresponding points in two images and computing the point depth based on the distance between corresponding points in the pair of images. It was reported that such a measurement tool has the highest accuracy among volume measurement approaches with the error rate less than 3%; however, it is costly and impractical in clinical application. Another investigation was used three progressive scan video cameras mounted on a triangle frame and a light projector placed at the centre of the rig holding the cameras called MEDPHOS (Medical Digital Photogrammetric System) measure volume of the pressure sores in which image triplets were acquired from the wound, followed by generation of three digital surface models that then combined to increase the reliability of generated

surface model. Finally, the volume of the wound, the space sandwiched between the measured surface of the wound and the original healthy skin surface, was calculated [49]. Another research team worked on the same setting with a novel strategy in characterizing the point correspondences along with their performance evaluation resulted in 96.8% robust 3D point reconstruction [39]. Apart from high accuracy level, it failed to measure the moist wounds with flat surface due to presence of reflection. Moreover, the calibration stage should be done by a trained operator and the fixed observation distance limited the field of view for large size wounds.

4.3.2 Wound 3d Analysis Using Structured Light

Using the colour coded structured light in wound assessment was proposed by Plassmann [29] which was then commercialized as MAVIS I (Measurement of Area and Volume Instrumentation System) in 1998, wherein a set of 70 parallel beams of varying colours was projected onto the wound surface and recorded by a CCD camera. Then a computer calculated 3D map of the wound from the position information of the focal points of projector and camera, and from the intersection points of the stripes of light with the wound surface. The error rate of this instrument was 3-5% for wounds with the size of 0.5-30 cm^2, but it was expensive and needs trained operator. The newer prototype, MAVIS II, was introduced in 2006 that equipped to a reflex digital camera with special dual lens optics to record two images from different view-angles which removed the needs for exact camera positioning, made the prototype portable in clinical environment, and simplified image capturing; however, it was still costly.

In another study, the structured lights were produced by using LCD projection system and a CCD camera, to reconstruct the 3D surface of five wound phantoms with depth of 4-10 mm and width of 15-25 mm. The results were compared with the manual measurement and Saline infusion. Among three methods, the structured light showed the best repeatability (<10%) when the wound sides were not steep; however, the outcomes cannot be achieved through clinical practice due to the small number of studied wounds and complexity of real ulcers like DFUs which was not modelled in used phantoms [50].

Another original approach in 3D assessment of skin wounds was initiated by Albouy, Lucas [52] and then improved by Treuillet, Albouy [3] in which the wound 3D model was obtained from un-calibrated images recorded by a handheld digital camera with free zooming. In particular, an original matching scheme and self-calibrating algorithm were used to produce a dense and precise reconstruction from two colour images. It was demonstrated that the best configuration for image acquisition was between 15° and 30° for vergence of stereo-pair with global precision 3%.

4.4 Monitoring Wound Tissue Changes Using Digital Photography

Camera images were also utilized in quantitative assessment of tissue changes during the wound generation and healing procedures, i.e. the healing kinetics was evaluated though analysis of colour images over time. In an investigation with the aim of studying a new drug, four 8 mm skin blisters were induced on the forearms of eight healthy subjects; then the optical images of the wound site were recorded between day 1 and day 12. Two healing indices that were built on the wound area and colour changes were used as criteria for tissue comparison during healing. The results revealed that the mean of chromatic green (g) in rgb colour space, which is less sensitive to the intensity compared to the RGB colour space, showed the greatest ratio of variance among the other colour features [41].

In another research, the colour images were taken from induced pressure ulcers on the porcine with the aim of grading the wounds in terms of their severity. The outcomes demonstrated that visible colour changes in hue channel of Hue-Saturation-Value (HSV) colour space may be used as a criterion for distinguishing the wound severity provided that the elapsed time from the injury was known. Also, correlation analysis with histological information indicated that it can be used to evaluate the effectiveness of treatment regimen. However, the proposed method was not able to determine the grade of wound severity for wound older than 30 minute [40].

Optical images of donor sites, one treated with topical alginates and the other with petrolatum gauze, in 10 patients were taken from day 6 to day 12 post graft removal every 2 days. Then, the meaningful parameters measuring the wound colour and homogeneity changes were extracted; and those that had significant changes over time were selected to construct the linear healing function. The performance of the healing function was compared with the results of principal component analysis (PCA) [36].

Also, the induced pressure ulcers in guinea pigs were photographed by digital camera and scanned by high-frequency ultrasound scanner at day 3, 7, 14, and 21 to assess the pressure sore generation and healing processes. Then, the colour and textural features that significantly changed with time were extracted from optical and HFU images; respectively, followed by grouping into five categories as inputs for multi-layer perceptron neural network to classify the examination days. The results revealed that the features extracted from camera images were not able to distinguish the day 14 from day 21, and the HFU features were not able to differentiate days 3 and 21. However, information fusion of both imaging modalities using a fuzzy integral was able to differentiate all classes and would be applied as a viable tool for assessing the generation and healing processes in pressure ulcers. One major limitation of the study was the difference between real chronic and induced wounds in terms of severity, depth, and patient's characteristics which definitively changed the time pattern used in the study [19].

5 Limitations

All above reviewed studies were in agreement that the digital photography can be utilized as a non–invasive, quantitative, fast, and cost–effective technique in wound healing assessment; however, it is not able to depict the full extent of underlying tissue damage. Most of the studies evaluated the healing in acute experimental wounds induced on pigs or human wherein the wound severity, depth, size, and the healing phase sequential order were not necessarily follow the pattern in chronic wounds. In addition, the wound images should be taken under controlled environment which is impractical in everyday clinical practice; otherwise colour analysis and wound dimensional measurement will subjected to high error rate and produce grossly incorrect results. Also, much work still needs to be done to arrive at a reliable and simple calibration system that affects image data quality only minimally and is still easy to use.

6 Conclusion

Optical imaging has great potential for non–invasive and quantitative wound assessment by targeting the monitoring of healing progress. It can also be combined with the other imaging modalities like high frequency ultrasound imaging to provide comprehensive and accurate information on tissue dimensional and structural changes that may ameliorate patient discomfort by adopting proactive treatment regimen. Further work, however, is required to diminish the dependency on expert clinicians

and operator by developing standard protocols for wound border delineation and wound colour image calibration.

REFERENCES

[1] Shaw, J. and P.M. Bell, *Wound measurement in diabetic foot ulceration*. 2011: INTECH Open Access Publisher.

[2] Dyson, M., et al., *Wound healing assessment using 20 MHz ultrasound and photography.* Skin Research and Technology, 2003. **9**(2): p. 116-121.

[3] Treuillet, S., B. Albouy, and Y. Lucas, *Three-dimensional assessment of skin wounds using a standard digital camera.* IEEE Transactions on Medical Imaging, 2009. **28**(5): p. 752-762.

[4] Plassmann, P. and T. Jones, *MAVIS: a non-invasive instrument to measure area and volume of wounds.* Medical Engineering & Physics, 1998. **20**(5): p. 332-338.

[5] Galushka, M., et al. *Case-based tissue classification for monitoring leg ulcer healing*. in *18th IEEE Symposium on Computer-Based Medical Systems, 2005*. 2005. IEEE.

[6] Humbert, P., S. Meaune, and T. Gharbi, *Wound healing assessment.* Phlebolymphology, 2004. **47**: p. 312-319.

[7] Plassmann, P. and B. Belem, *Early Detection of Wound Inflammation by Color Analysis*, in *Computational Intelligence in Medical Imaging: Techniques and Applications*. 2009, CRC Press. p. 89-110.

[8] Belem, B., *Non-invasive wound assessment by image analysis*. 2004, University of Glamorgan.

[9] Hoppe, A., et al. *Computer assisted assessment of wound appearance using digital imaging*. in *Engineering in Medicine and Biology Society, 2001. Proceedings of the 23rd Annual International Conference of the IEEE*. 2001. IEEE.

[10] Kolesnik, M. and A. Fexa, *Multi-dimensional color histograms for segmentation of wounds in images*, in *Image Analysis and Recognition*. 2005, Springer. p. 1014-1022.

[11] Mukherjee, R., et al., *Automated tissue classification framework for reproducible chronic wound assessment.* BioMed Research International, 2014. **2014**: p. 1-9.

[12] Oduncu, H., et al., *Analysis of skin wound images using digital color image processing: a preliminary communication.* The International Journal of Lower Extremity Wounds, 2004. **3**(3): p. 151-156.

[13] Pinero, B.A., C. Serrano, and J.I. Acha. *Segmentation of burn images using the L* u* v* space and classification of their depths by color and texture imformation*. in *Medical Imaging Conference*. 2002. International Society for Optics and Photonics.

[14] Veredas, F., H. Mesa, and L. Morente, *Binary tissue classification on wound images with neural networks and bayesian classifiers.* IEEE Transactions on Medical Imaging, 2010. **29**(2): p. 410-427.

[15] Wannous, H., Y. Lucas, and S. Treuillet, *Enhanced assessment of the wound-healing process by accurate multiview tissue classification.* IEEE Transactions on Medical Imaging, 2011. **30**(2): p. 315-326.

[16] Jones, T.D. and P. Plassmann, *An active contour model for measuring the area of leg ulcers.* IEEE Transactions on Medical Imaging, 2000. **19**(12): p. 1202-1210.

[17] Krouskop, T.A., R. Baker, and M.S. Wilson, *A noncontact wound measurement system.* Journal of Rehabilitation Research and Development, 2002. **39**(3): p. 337-346.

[18] Liu, X., et al., *Wound measurement by curvature maps: a feasibility study.* Physiological Measurement, 2006. **27**(11): p. 1107-1123.

[19] Moghimi, S., M.H.M. Baygi, and G. Torkaman, *Automatic evaluation of pressure sore status by combining information obtained from high-frequency ultrasound and digital photography.* Computers in Biology and Medicine, 2011. **41**(7): p. 427-434.

[20] Moghimi, S., et al., *Quantitative assessment of pressure sore generation and healing through numerical analysis of high-frequency ultrasound images.* Journal of Rehabilitation Research and Development, 2010. **47**: p. 99-108.

[21] Romanelli, M., et al., *Technological advances in wound bed measurements.* WOUNDS-A COMPENDIUM OF CLINICAL RESEARCH AND PRACTICE, 2002. **14**(2): p. 58-66.

[22] Unger, P., C. Fife, and D. Weir, *Capturing the essence of the wound evaluation.* Today's Wound Clinic, 2008: p. 38-42.

[23] Tallman, P., et al., *Initial rate of healing predicts complete healing of venous ulcers.* Archives of dermatology, 1997. **133**(10): p. 1231-1234.

[24] Kantor, J. and D. Margolis, *A multicentre study of percentage change in venous leg ulcer area as a prognostic index of healing at 24 weeks.* British Journal of Dermatology, 2000. **142**(5): p. 960-964.

[25] Flanagan, M., *Wound measurement: can it help us to monitor progression to healing?.* Journal of Wound Care, 2003. **12**(5): p. 189-194.

[26] Charles, H., *Wound assessment: measuring the area of a leg ulcer.* British Journal of Nursing, 1998. **7**(13): p. 765-772.

[27] Gethin, G., *The importance of continuous wound measuring.* WOUNDS UK, 2006. **2**(2): p. 60.

[28] Bulstrode, C., A. Goode, and P. Scott, *Stereophotogrammetry for measuring rates of cutaneous healing: a comparison with conventional techniques.* Clinical Science (Lond), 1986. **71**(4): p. 437-43.

[29] Plassmann, P., *Measuring wounds.* Journal of Wound Care, 1995. **4**(6): p. 269-272.

[30] Wendelken, M., et al., *Wounds measured from digital photographs using photodigital planimetry software: validation and rater reliability.* Wounds: A Compendium of Clinical Research and Practice, 2011. **23**(9): p. 267-275.

[31] Cuzzell, J.Z., *The new RYB color code.* The American Journal of Nursing, 1988. **88**(10): p. 1342-1346.

[32] Zheng, H., et al. *New protocol for leg ulcer tissue classification from colour images*. in *26th Annual International Conference of the IEEE, Engineering in Medicine and Biology Society*. 2004. IEEE.

[33] Wannous, H., S. Treuillet, and Y. Lucas. *Supervised tissue classification from color images for a complete wound assessment tool*. in *29th Annual International Conference of the IEEE, Engineering in Medicine and Biology Society*. 2007. IEEE.

[34] Jones, B.F. and P. Plassmann, *An instrument to measure the dimensions of skin wounds.* IEEE Transactions on Biomedical Engineering, 1995. **42**(5): p. 464-470.

[35] Nischik, M. and C. Forster, *Analysis of skin erythema using true-color images.* IEEE Transactions on Medical Imaging, 1997. **16**(6): p. 711-716.

[36] Bon, F.X., et al., *Quantitative and kinetic evolution of wound healing through image analysis.* IEEE Transactions on Medical Imaging, 2000. **19**(7): p. 767-772.

[37] Perez, A.A., A. Gonzaga, and J.M. Alves. *Segmentation and analysis of leg ulcers color images*. in *Medical Imaging and Augmented Reality, 2001. Proceedings. International Workshop on*. 2001. IEEE.

[38] Berriss, W.P. and S.J. Sangwine *A colour histogram clustering technique for tissue analysis of healing skin wounds*. IET Conference Proceedings, 1997. 693-697.

[39] Malian, A., et al., *Development of a robust photogrammetric metrology system for monitoring the healing of bedsores.* The Photogrammetric Record, 2005. **20**(111): p. 241-273.

[40] Hansen, G.L., et al., *Wound status evaluation using color image processing.* IEEE Transactions on Medical Imaging, 1997. **16**(1): p. 78-86.

[41] Herbin, M., et al., *Assessment of healing kinetics through true color image processing.* IEEE Transactions on Medical Imaging, 1993. **12**(1): p. 39-43.

[42] Plassmann, P. and T.D. Jones, *Improved active contour models with application to measurement of leg ulcers.* Journal of Electronic Imaging, 2003. **12**(2): p. 317-326.

[43] Zhang, Z., W.V. Stoecker, and R.H. Moss, *Border detection on digitized skin tumor images.* IEEE Transactions on Medical Imaging, 2000. **19**(11): p. 1128-1143.

[44] Karkanis, S.A., et al., *Computer-aided tumor detection in endoscopic video using color wavelet features.* IEEE transactions on information technology in biomedicine, 2003. **7**(3): p. 141-152.

[45] Cula, O.G., et al., *Skin texture modeling.* International Journal of Computer Vision, 2005. **62**(1-2): p. 97-119.

[46] Resch, C.S., et al., *Pressure sore volume measurement: a technique to document and record wound healing.* Journal of the American Geriatrics Society, 1988. **36**(5): p. 444-446.

[47] Thomas, A.C. and A.B. Wysocki, *The Healing Wound: A Comparison of Three Clinicially Useful Methods of Measurement.* Advances in Skin & Wound Care, 1990. **3**(1): p. 18.

[48] Langemo, D.K., et al., *Comparison of 2 wound volume measurement methods.* Advances in skin & wound care, 2001. **14**(4, Part 1 of 2): p. 190-196.

[49] Boersma, S.M., et al., *Photogrammetric wound measurement with a three-camera vision system.* International Archives of Photogrammetry and Remote Sensing, 2000. **33**(B5/1; PART 5): p. 84-91.

[50] Ozturk, C., et al. *A new structured light method for 3-D wound measurement*. in *IEEE Twenty-Second Annual Northeast Bioengineering Conference*. 1996. IEEE.

[51] Callieri, M., et al. *Derma: Monitoring the Evolution of Skin Lesions with a 3D System*. in *VMV*. 2003.

[52] Albouy, B., Y. Lucas, and S. Treuillet. *3D Modeling from uncalibrated color images for a complete wound assessment tool*. in *29th Annual International Conference of the IEEE, Engineering in Medicine and Biology Society*. 2007. IEEE.

SOCIETY FOR SCIENCE AND EDUCATION
UNITED KINGDOM

JBEMi JOURNAL OF BIOMEDICAL ENGINEERING AND MEDICAL IMAGING

ISSN : 2055-1266
VOLUME 3 NO. 5

Left Sided Mc Connells Sign: A Classic Finding in a Rare Condition

Eric McWilliams, Ehab Amer and Ali Alshehri
Cardiology Department, Johns Hopkins Aramco Healthcare, Dhahran, Saudi Arabia
eric.mcwilliams@gmail.com; amerehab@hotmail.com; ehab.amer@jhah.com

A 32 year old lady with a history of systemic lupus erythematosus (SLE) complicated by crescentic lupus nephritis and end stage renal failure on thrice weekly haemodialysis, presented to the emergency department with breathlessness, chest pain and haemoptysis, stating that her symptoms had started roughly 24 hours earlier. She appeared anxious and in distress. BP was 160/105 mmHg, heart rate 105/min and there was evidence of bilateral rales and a gallop rhythm. She was afebrile but only 94% saturating on high flow oxygen.

ECG showed left ventricular hypertrophy and non-specific changes, chest X-ray demonstrated bilateral patchy infiltrates and cardiomegaly(figure 1). White cell count was 13.7 K, CRP 2.1, Creatinine 8.6, BUN 46, K 4.6 and high sensitivity troponin elevated at 8.755 (ref < 0.03).

Echocardiography (Video 1) showed severe hypokinesis of the septum, anterior wall and basal inferior wall with an estimated ejection fraction of 40 % but preserved or even hyperkinetic apical function. (figure 1 & Video 2) There was evidence of high filling pressures and pulmonary hypertension. (figure 2) Speckle tracking echo (STE) demonstrated preserved apical strain (figure 2) with markedly reduced strain in the basal segments.

A presumptive diagnosis of basal variant Taku tsubo cardiomyopathy was made and the patient admitted to the intensive care unit. She was treated by emergent haemodialysis and was commenced on betablockade in the form of Carvedilol. She demonstrated rapid clinical improvement. She declined invasive workup with coronary angiography. There were no significant serial EKG changes.

Repeat echocardiography (Video 3&4)was performed 48 after presentation and demonstrated normalisation of LV systolic function as well marked improvement in diastolic parameters (Figure 3).Speckle tracking echo also showed marked improvement in comparison with the echo on presentation(Figure 4). At this stage, the patient insisted on discharge and she has remained well at follow up. In retrospect, she admitted that she had become distraught with a work colleague during an argument immediately before her symptoms commenced. The rapid recovery of LV function and the non-coronary distribution of LV dysfunction excludes other aetiologies such as coronary embolism, plaque rupture or dissection.

The echocardiogram shows classic basal type taku tsubo cardiomyopathy(TTC), with preserved apical function. Four distinct variants of TTC have been described. Basal type TTC is rare and reported in 2.2% of TTC cases (39 of 1750 cases) in the international TTC registry[1]. Apical type is the commonest 81.7%;

DOI: 10.14738/jbemi.35.2190
Publication Date: 17th September 2016
URL: http://dx.doi.org/10.14738/jbemi. 35.2190

midventricular type occurs in 14.6% and focal is rare occurring in only 1.5%[1]. TTC can occur in younger females but the risk is 4.8% greater in females >55 years. The traditional wisdom is that TTC is often precipitated by emotional stress but physical factors actually predominated as the commonest precipitating factor in the international registry.[1]

The diagnosis of TTC is usually confirmed by the exclusion of significant obstructive coronary artery disease by invasive angiography, particularly in patients presenting with a syndrome suggesting ACS. However, it may not always be possible to perform coronary angiography and echocardiography plays a pivotal role in the diagnosis, risk stratification and follow up of TTC patients.[2] Advanced echocardiographic techniques such as STE, myocardial contrast and coronary flow studies may be incorporated into an algorithm than can obviate the need for invasive angiography in some patients.[2]

McConnell's sign is a specific finding in cases of acute pulmonary embolism. Mc Connells sign[3] is defined as right ventricular free wall akinesis with sparing of RV apical contraction and is considered a specific echocardiographic finding in acute pulmonary embolism.

The presence of hyperkinetic motion of the basal and mid segments of the RV free wall with RV apical akinesis suggests right ventricular involvement in TTC and this finding has been suggested as "reverse McConnell's sign".[4] LV apical hyperkinesis with basal and midventricular hypokinesis could be considered a "left sided Mc Connell's sign" and should suggest basal or midventricular variants of TTC.

Disclosures:

None of the authors have any disclosures.

REFERENCES

[1] Clinical Features and outcomes of Taku Tsubo (stress) Cardiomyopathy:n engl j med 373;10 nejm.org September 3, 2015

[2] Standard and Advanced Echocardiography in Taku Tsubo (Stress) Cardiomyopathy: Clinical and Prognostic Implications. j.echo.2014.08.020

[3] Regional right ventricular dysfunction detected by echocardiography in acute pulmonary embolism. McConnell MV, Solomon SD, Rayan ME, Come PC, Goldhaber SZ, Lee RT. Am J Cardiol. 1996 Aug 15;78(4):469-73.

[4] "Reverse McConnell's Sign?": A Unique Right Ventricular Feature of Takotsubo Cardiomyopathy: Kan Liu, MD, PhD Robert Carhart, MD. AM J Cardiol.2013 April 15; 111, Issue 8: 1232–1235

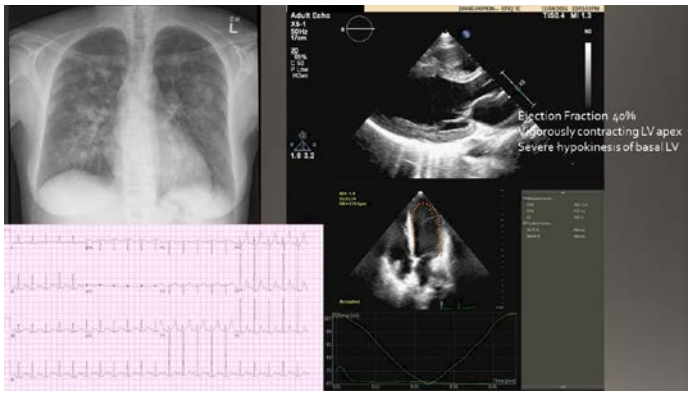

Figure 1: Panel A: Chest X-ray showing pulmonary edema. Panel B: EKG. Panel C: Transthoracic echo PLAX view at presentation. Panel D: initial echo apical view

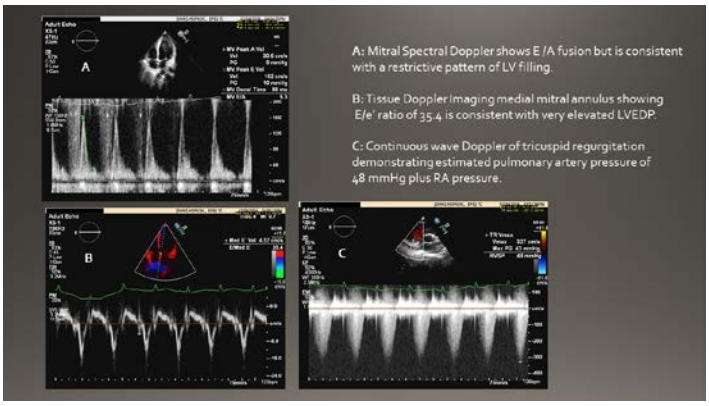

Figure 2: Echo Doppler findings at presentation. Panel A: pulsed Doppler mitral inflow. Panel B: tissue Doppler septal annulus. Panel C: continuous wave Doppler tricuspid valve

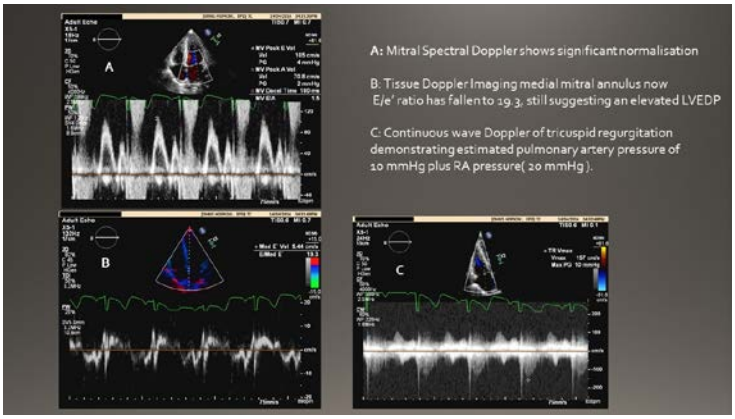

Figure 3: Echo Doppler findings at 48 hours. Panel A: pulsed Doppler mitral inflow. Panel B: tissue Doppler septal annulus. Panel C: continuous wave Doppler tricuspid valve

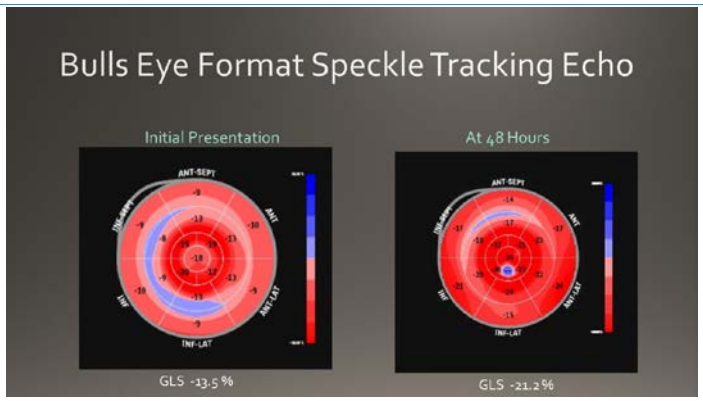

Figure 4: Speckle tracking echo in bulls eye format demonstrating longitudinal strain. Left panel at presentation. Right panel after 48 hours.

VIDEOS

Video 1: Transthoracic echo, parasternal long axis view at presentation
http://scholarpublishing.org/Repository/JBEMi/Video1.wmv

Video 2: Transthoracic echo, apical 4 chamber view at presentation
http://scholarpublishing.org/Repository/JBEMi/Video2.wmv

Video 3: Transthoracic echo, parasternal long axis view at 48 hours
http://scholarpublishing.org/Repository/JBEMi/Video3.wmv

Video 4: Transthoracic echo, apical 4 chamber view at 48 hours
http://scholarpublishing.org/Repository/JBEMi/Video4.wmv

SOCIETY FOR SCIENCE AND EDUCATION
UNITED KINGDOM

JBEMi JOURNAL OF BIOMEDICAL ENGINEERING AND MEDICAL IMAGING

ISSN : 2055-1266
VOLUME 3 NO. 5

Magnetic Resonance T2 Relaxometry In Knee Joint Patellar Cartilage Imaging

[1]Raj Kumar Soundarajan, [2]Rajeswaran R and [3]Sheila Elangovan
[1]Aster Hospital, DM Health group, Dubai, UAE
[2,3]College of Allied Health Sciences, Department of Radiology and Imaging Sciences, Sri Ramachandra University, Chennai, India
[1]rajpmakumar@icloud.com

ABSTRACT

Background: Over the past decade the diagnosis of knee disorders has improved significantly through better imaging techniques. Imaging of the Knee joint includes Radiograph, Computed Tomography, Magnetic Resonance Imaging, Arthrography and of advanced imaging techniques like T2 Relaxometry.

Aim: To obtain T2 relaxometry value of knee joint patellar cartilages & to compare the T2 relaxometry values of the Osteoarthritic patients with that of the other cause.

Material & Methods: 20 patients who presented themselves in Radiology department of either sex whose reports and image data's are collected prospectively during the study period of December 2011 to February 2012. All the patients' data within the study period were collected. Patients were selected irrespective of their age group, gender and pathologic findings, a detailed history with various patient's data includes patient demography, age, sex and the study reports are collected and is entered in a specially designed Profoma. The acquired study data of Sagittal T2 Mapping High Resolution sequence of each patient are then post processed by using a GE Advantage Workstation (version 4.4) and T2 Relaxometry values of various knee joint cartilages (Medial Patellar cartilage, Lateral Patellar cartilage) are collected by using a special software and is entered in the Profoma table.

Conclusion: Conventional MRI may not show early cartilage changes; Cartilage edema following trauma (or) Due to osteoarthritis can be picked up early by T2 Mapping. hence it is useful in early patient management.

***Key words*:** MRI, Knee joint imaging, Patellar Imaging, T2 Relaxometry, T2 Mapping, osteoarthritis, Knee trauma.

1 Introduction

Over the past decade the diagnosis of knee disorders has improved significantly through better imaging techniques. Imaging of the Knee joint includes Plain Radiograph, Computed Tomography (CT), Magnetic Resonance Imaging (MRI), Arthrography and of advanced imaging techniques like T2 Relaxometry. Radiographs of the knee are usually the first imaging studies, especially if bone wear and tear is suspected clinically. Radiographs are often required after acute trauma. The most common views are

DOI: 10.14738/jbemi.35.2251
Publication Date: 09th October 2016
URL: http://dx.doi.org/10.14738/jbemi. 35.2251

the Antero Posterior (AP), the Lateral, and the Skyline view. Early changes in the cartilage and other articular tissues are not directly visible. In Computed Tomography, axial images were obtained and can be reformatted into sagittal and coronal planes. It also allows 3 dimensional (3D) reconstruction of knee joint and is very useful in case of trauma, fractures, etc. It provides good details about bony structures with less tissue contrast when compared to that of MRI.

1.1 Magnetic Resonance Imaging:

MR imaging is a powerful tool for the morphologic and compositional imaging of cartilage in the knee. MRI offers multi-planar capabilities, high spatial resolution without ionizing radiation, and superior contrast between joint tissues. For routine clinical examinations of the knee joint, most departments are still applying a multiplane 2D fast SE sequence, alone or in combination with a 3D GRE sequence to improve cartilage assessment. The combined use of high-resolution morphologic imaging techniques and compositional imaging techniques may lead to increased sensitivity of MR imaging for the detection of early cartilaginous degeneration and increased utility for the assessment of cartilage repair techniques.

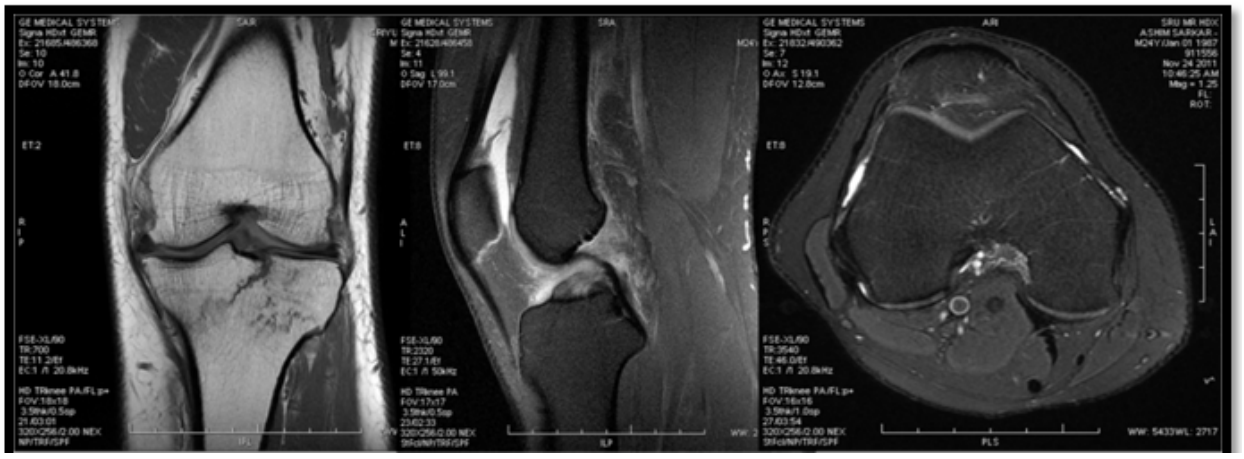

Figure 1: MRI – Coronal T1 / Sagittal /Axial Proton Density with Fat Suppression

1.2 T2 Mapping:

T2 relaxation time is a non-invasive marker of cartilage degeneration because it is sensitive to tissue hydration and biochemical composition. When collagen breaks down, there is increased mobility of water in the cartilage and therefore a prolongation in T2 relaxation times. It is based on a multi-echo pulse sequence derived from the existing FSE-XL that can create up to 8 echoes per single acquisition not more than eight echoes are acquired, due to the cartilage short T2 relaxation times. Cartigram automatically generates color-maps based on a scale of T2 values that allows visualization of changes in the composition of articular cartilage in some cases before changes in the thickness can be seen.

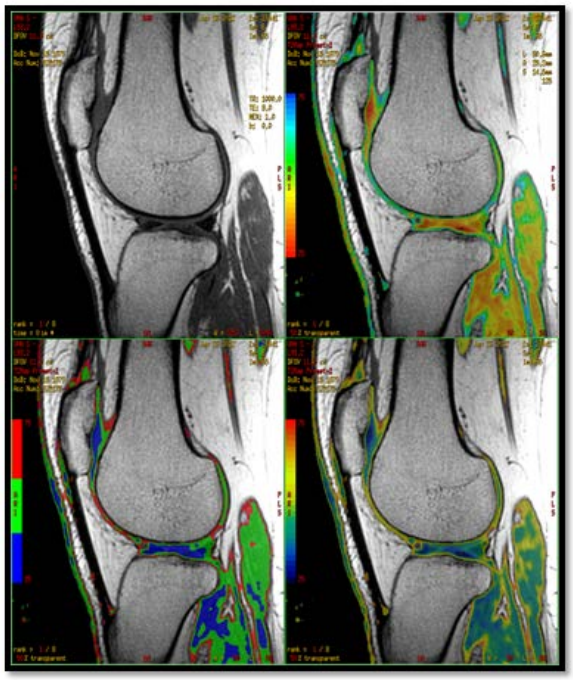

Figure 2: MR-T2 Mapping Sagittal plane

2 AIM

- To obtain T2 relaxometry value of knee joint patellar cartilages
- To compare the T2 relaxometry values of the Osteoarthritic patients with that of the other cause.

3 Anatomy of The Knee

The knee joint is the largest synovial joint in the body. It consists of the articulation between the femur and tibia, which is weight bearing; and the articulation between the patella and the femur, which allows the pull of the quadriceps femoris muscle to be directed anteriorly over the knee to the tibia without tendon wear. two fibrocartilaginous menisci, one on each side, between the femoral condyles and tibia accommodate the changes in the shape of the articular surfaces during joint movements. The detailed movements of the knee joint are complex, but basically the joint is a hinge joint that allows mainly flexion and extension.

The major cartilages associated with the knee joint are 1, The Patellar Cartilage, 2, The Collateral Cartilages & 3, The Cruciate Cartilages.

3.1 Patellar Cartilage

The Patellar cartilage is basically the continuation of the quadriceps femoris tendon inferior to the patella. It is attached above to the margins and apex of the patella and below to the tibial tuberosity.

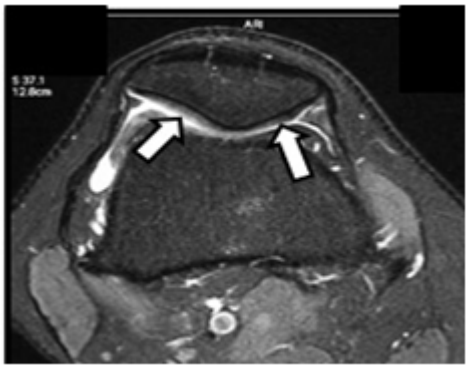

Figure 3: MRI Axial Image shows cross section of patellar cartilage (white arrows)

4 PROTOCAL - MRI OF KNEE

Exclusive MRI screened has done to all patients with metal detector before the procedure to avoid complications due to any implants. Possible contra-indications must be checked. Metallic jewelers should be removed prior to MR examinations as it because RF burns due to high RF absorption locally; The MR imaging sequences most commonly used in the assessment of joint cartilage are 2D or multisection T1-weighted, proton density–weighted and T2-weighted imaging sequences with or without fat suppression.

4.1 PATIENT POSITIONING: Patient was made to lay down in Supine position with The knee in the center of the coil with the external rotation of 15^0 to 20^0, flexed to 5^0 to 10^0 and the coil was closed after adequate immobilization and the landmark was set in the center of the coil.

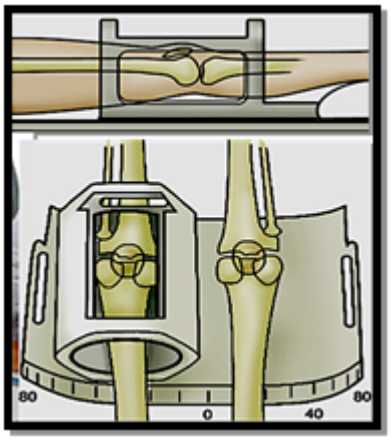

Figure 4: Positioning for MRI Knee joint

5 Material and Methods

A population of 20 subjects who presented themselves in Sri Ramachandra Hospital (A tertiary care university hospital in Chennai, India) to the Department of Radiology and Imaging Sciences of either sex whose reports and image data's are collected prospectively during the study period of 3 months (December 2011- February 2012). All the patients' data within the study period were collected. Patients were selected irrespective of their age group, gender and pathologic findings. A detailed history with various patient's data includes patient demography, age, sex and the study reports are also collected and is entered in a specially designed Profoma.

5.1 Materials:

The GE Signa HDx MRI system (1.5T) whole body magnetic resonance scanner with the 8 channel, 9-element phased-array knee coil is used for imaging. The MR imaging sequences most commonly used in the assessment of joint cartilage are 2D or multisection sagittal & axial (FSE) Proton Density Weighted with Fat Suppression (PD FS), sagittal gradient echo sequence, T2 weighted Fast Spin Echo, T1 weighted (T1w SE)and coronal Shot TAU Inversion Recovery (STIR); In addition to the routine protocol the ***T2 Mapping*** sequence is added.

5.2 T2 Mapping:

Routine MR imaging allows a subjective assessment of cartilage T2 changes, whereas quantitative T2 mapping provides objective data by generating either a color or a gray-scale map representing the variations in relaxation time within cartilage. A multiecho SE technique is used to measure T2 values. T2 Map acquires multiple scans at each location; each set of scans has a unique TE, resulting in a data set of images that represent different T2 weighting. The number of TEs per scan (not a selectable parameter) is the scan parameter that determines the number of images that are acquired at each location. For example, if 10 locations are prescribed with 8 TEs per scan, then there are 10 data sets with 8 images per location. Each image within a data set or location has 8 unique T2-weighted images, because all lines of k-space are filled with one TE. The data is processed in ***Functool,*** producing T2 color maps to visualize the changes in cartilage that are not visible in gray scale MR images. In MRI T2 decay imaging of hyaline articular cartilage reflects interactions among water molecules and between water molecules and surrounding macromolecules and is highly sensitive to alterations of the cartilage matrix. Increased interactions between water and macromolecules such as those of collagen result in decreased T2. Thus, T2 is highly sensitive to changes in hydration (or, nearly equivalently, collagen concentration) and in the normally anisotropic orientation of the collagen fibrils within the extracellular cartilage matrix (50) that result from physiologic or pathophysiologic processes in cartilage. In normal cartilage, regional and zonal differences in density and organization of the collagen matrix appear as variations in T2. There is good evidence that T2 mapping is useful for identifying sites of early-stage degeneration (early disruption of the collagen matrix) in cartilage, which appear as areas with T2 higher than that of normal cartilage.

Figure 5: T2 Mapping sequence - T2 images with 8 TEs (ms) – 8.9, 17.8, 28.7, 35.6, 44.4, 53.3, 62.2, 71.1With the generated T2 Color Map (center image)

5.3 Applications:

T2 Map is used to image cartilage. Healthy collagen, which has a short T2 relaxation time, is a highly-organized, anisotropic structure that restricts the flow of water. The body uses this cushion of water to absorb shock. The T2 relaxation time of articular cartilage is a function of the water content of the tissue. An increase in T2 relaxation times within cartilage has been associated with matrix damage, especially loss of collagen matrix. The T2 Map and the parametric images produce visible image contrast changes (T1 and T2 alterations) in early stages of cartilage degeneration, such as osteoarthritis.

Table 1: Protocol for T2 Mapping – Sagittal plane

PARAMETERS	
Scan plane	Sagittal
Mode	2D
Pulse sequence family	Spin echo
Pulse sequence	FSE-T2
TR (ms)	1000
TE (ms)	(1)08.9, (2)17.8, (3) 26.7, (4)35.6,(5) 44.4, (6) 53.3, (7)62.2, (8)71.2
FOV (cm)	16 x 16
Slice thickness (mm)	2
Spacing (mm)	4
Flip angle (degree)	90
Frequency	288
Phase	224
NEX	1
Scan time	3:46 min

5.4 Post Processing:

Functool is software package that allows the analysis of MR data sets for post processing. The images can represent changes in image intensity over time, b–value or gradient orientation (diffusion imaging), or frequency (spectroscopy). Results are in the form of graphs and functional maps that can be saved & documented.

5.4.1 : T2 Mapping Functool:

T2 MAP protocol post processes data sets acquired using the T2Map application. The T2Map acquisition is displayed in Functool where the T2 relaxation time color map is coded to capture T2 values from the TE range of the acquired images.

1. The source image is displayed in the upper left Map viewport
2. The T2Map Preset-1 parametric image is displayed in the lower left viewport.
3. The T2Map Preset-2 parametric map is displayed in the lower right viewport.

4. A curve displaying signal intensity on the vertical axis and the echo number on the horizontal axis is displayed in the upper right viewport. A data point for each echo is plotted when an ROI is deposited on any of the three images.

T2Map layout is comprised of 4 viewports

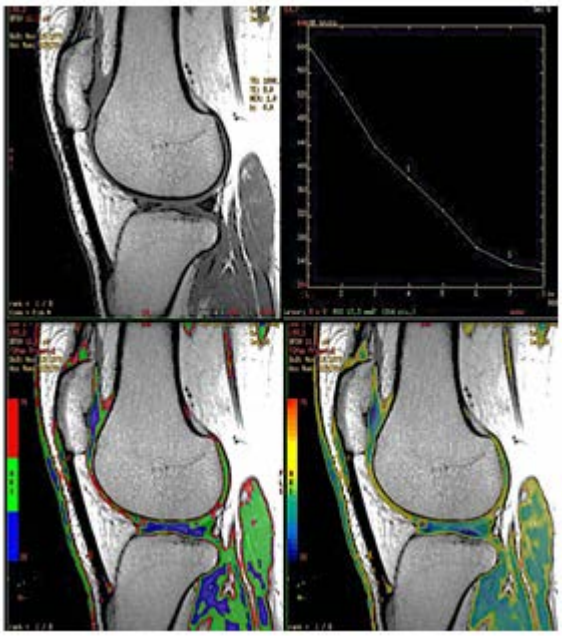

Figure 6: T2 Mapping layout in Functool application (Version: ADW4.4GE workstation)

5.4.2: T2 Mapping Workflow

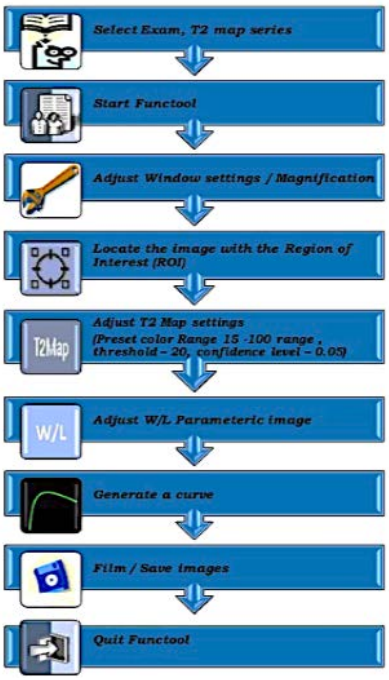

5.5 Interpretation of The Color Mapping:

The parametric map color scheme is as follows:

- Short T2 structures = Orange to Red
- Intermediate T2 structures = Yellow
- Long T2 structures = Green to Blue

6 Observations and Result

The post processing of MR Cartigram (Sagittal) of 20 patients on the Functool reveals the following results.

In this study we calculated the T2 relaxation times of the cartilages, and found that there is an increase in those values due to various reasons, and thus commercial MR imaging has been used to confirm the diagnosis. It allows a subjective assessment of cartilage T2 changes, whereas quantitative T2 mapping provides objective data by generating either a color or a gray-scale map representing the variations in relaxation time within cartilage. A multiecho SE technique is used to measure T2 values. T2 Mapping acquires multiple scans at each location; each set of scans has a unique TE, resulting in a data set of images that represent different T2 weighting.

The data is processed in ***FuncTool,*** producing T2 color maps to visualize the changes in cartilage that are not visible in gray scale MR images. In our study,

- Out of 9 patients with the history of trauma there is an increase in the T2 relaxometry values for 6 patients.
- Out of 7 patients with the history of unknown knee pain shows increase in the T2 relaxometry values for 5 patients.
- Patients with history of knee instability/ pain on action and others (No. of patients 2/1/1 respectively) shows less significant increase in the T2 Relaxation time.

On comparing the T2 Relaxometry values of the patients with the history of Osteoarthritis vs. others, shows an increase in the T2 relaxation time of the knee joint cartilages. This is due to the early morphological changes occurs due to osteoarthritis in the knee joint cartilages.

There is good evidence that T2 mapping is useful for identifying sites of early-stage degeneration (early disruption of the collagen matrix) in cartilage.

Table 2: Comparison of T2 relaxometry values of Osteoarthritis and other patients

OSTEOARTHRITIS	6
OTHERS CONDITIONS	14

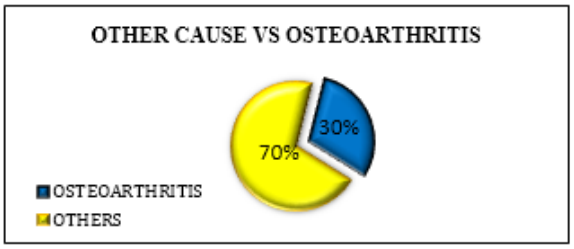

Graph 1: Percentage of T2 relaxometry values of Osteoarthritis over other patients

Table 3: Clinical symptomatology for other patients

CLINICAL SYMPTOMS	NO. OF PATIENTS	PERCENTAGE (%)
Trauma	9	45
Rest Pain	7	35
Instability	2	10
Pain On Activity	1	5
POLIO	1	5

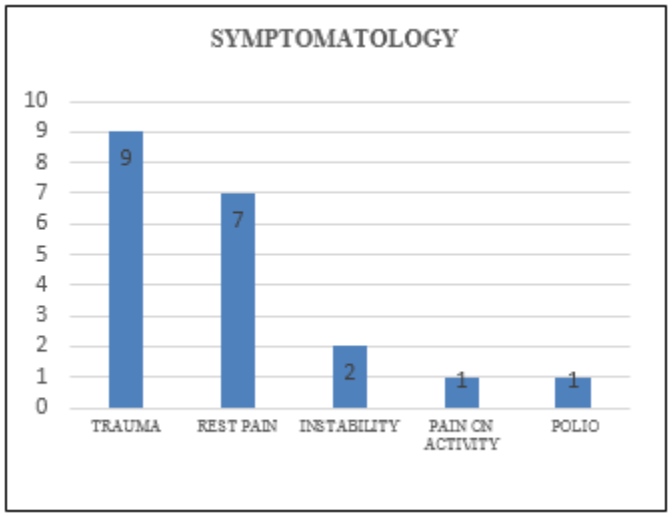

Graph 2: Distribution of other patient's symptomatology

Table 3 shows the clinical symptoms of the patients who came for MRI Knee Joint

This graph shows that 45% of the patients are with the history of trauma, followed by rest pain that is around 35 %, then with the knee instability 10 %, and with least symptoms of pain on action & with polio disorder of 5 % each

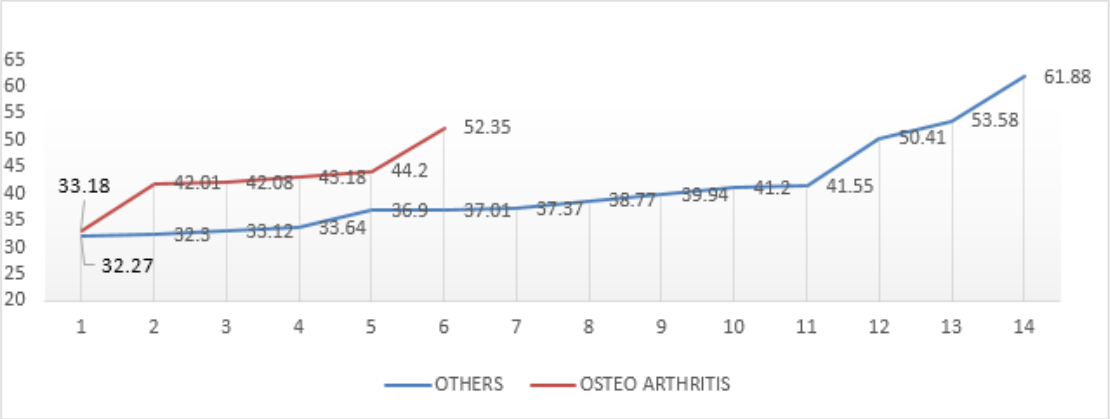

Graph 3: Comparison of T2 relaxometry values of the medial Patellar Cartilage in osteoarthritis patients and in other symptoms.

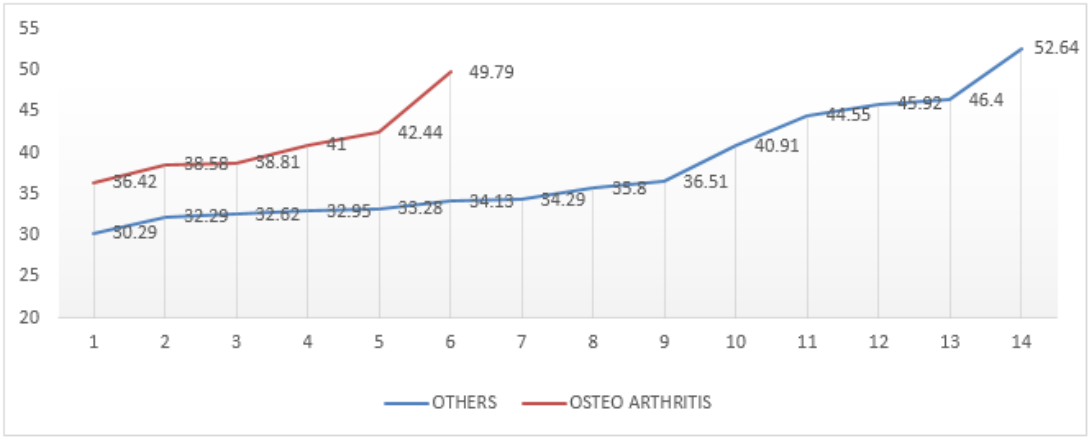

Graph 4: Comparison of T2 relaxometry values of the lateral Patellar Cartilage in osteoarthritis patients and in other symptoms.

7 Conclusion

Cartilage edema following trauma (or) Due to osteoarthritis can be picked up early by MR Cartigram. Conventional MRI may not show early cartilage changes hence T2 Mapping is useful in patient management. T2 mapping can be implemented relatively on most clinical MR imaging systems, as pulse sequences for obtaining quantitative T2 maps and software for generating colour T2 maps are now available in commercial packages.

REFERENCES

[1] Crema MD, Roemer FW, Marra MD, Burstein D, Gold GE, Eckstein F, Baum T, Mosher TJ, Carrino JA, Guermazi A. Articular cartilage in the knee: current MR imaging techniques and applications. Radiographics - .Jan-Feb 2011.

[2] Sharmila Majumdar and Blumenkrantz on Quantitative Magnetic Resonance Imaging Of Articular Cartilage In Osteoarthritis.

[3] C. Liess, S. Lu¨Sse, N. Karger, M. Heller and C.-C. Glu¨Er - On the detection of changes in cartilage water content using MRI T2-Mapping.

[4] Tallal C. Mamisch MD, Siegfried Trattnig MD, Sebastian Quirbach MD, Stefan Marlovits MD, Lawrence M. White MD, Goetz H. Welsch, on the Quantitative T2 Mapping of knee cartilage: Differentiation of healthy control cartilage and cartilage repair tissue in the knee with unloading.

[5] Jinfa Xu, Guohua Xie, Yujin Di, Min Bai, Xiuqin Zhao on The Value Of T2-Mapping and DWI in the Diagnosis Of early Knee cartilage injury.

[6] Garry E. Gold, Christina A. Chen,Seungbum, Brian A. Hargreaves, Neal K. Bangerters on Recent Advances in MRI of Articular Cartilage.

[7] Klaus M. Friedrich, Timothy Shepard, Valesca Sarkis De Oliveira, Ligong Wang, James S. Babb, Mark Schweitzer, Ravinder Regatte on the T2 measurements of cartilage in osteoarthritis patients with meniscal tears.

[8] Iwan Van Breuseghem, , Hilde T. C. Bosmans, , Luce Vander Els, Frederik Maes, on the Feasibility of T2 Mapping of human femoro-tibial Cartilage With Turbo Mixed MR Imaging at 1.5 T.

[9] Catherine Westbrook MRI IN PRACTICE – Third Edition.

[10] Alfred L. Horowitz, MRI Physics for Radiologist – Second Edition.

[11] Gray's Anatomy for students – Second Edition.

